EurJIC
European Journal of Inorganic Chemistry

A Journal of ChemPubSoc Europe

Accepted Article

Title: Pyridine-stabilized rhodium nanoparticles in ionic liquid as selective catalysts in hydrogenation and transfer hydrogenation processes

Authors: Alejandro Serrano-Maldonado, Erika Martin, and Itzel Guerrero-Ríos

To be cited as: *Eur. J. Inorg. Chem.* 10.1002/ejic.201900223

Link to VoR: http://dx.doi.org/10.1002/ejic.201900223

WILEY-VCH

10.1002/ejic.201900223

WILEY-VCH

FULL PAPER

Pyridine-stabilized rhodium nanoparticles in ionic liquid as selective catalysts in hydrogenation and transfer hydrogenation processes

Alejandro Serrano-Maldonado,[a] Erika Martin[†][a] and Itzel Guerrero-Ríos*[a]

[†]In memory of Prof. Erika Martin (1963-2017)

Rhodium nanoparticles (RhNPs) stabilized with pyridine-based ligands in the ionic liquid [BMIM][BF_4] (**RhNPs-I** to **III**) were synthesized from the organometallic precursor [Rh(μ-OMe)COD]$_2$ under dihydrogen pressure. The pyridine-stabilized RhNPs showed smaller size compared to the ligand free **RhNPs-V** and presented higher activity and selectivity in the hydrogenation of acetophenone to 1-phenylethanol. In the case of pyridine-capped **RhNPs-I**, the system was reused for several runs without loss of activity and selectivity. Nitrobenzene was reduced to aniline with dihydrogen in the presence of **RhNPs-I** with moderate activity. When the hydrogen source was formic acid-Et_3N azeotrope (transfer hydrogenation) the reaction was completed within minutes with high selectivity. Under transfer hydrogenation conditions, it was possible to apply the catalytic system **RhNPs-I** in multistep processes for the generation of substituted arylic amines through the reductive *N*-alkylation of nitrobenzene and benzaldehyde; and the synthesis of substituted pyrroles through the nitroarene reduction/Paal-Knorr condensation.

Introduction

Today, many industrial processes rely on rhodium catalysts due to its extraordinary and often unique catalytic properties. Rhodium nanoparticles (RhNPs) as catalysts have emerged as a strategy to improve the catalytic performance.[1,2] RhNPs combine the advantages of homogeneous and heterogenous catalysts, performing chemical transformations under mild conditions due to their high surface area. The possibility of catalyst reutilization is especially favored when ionic liquids (ILs) are employed as stabilizing agents and reaction media.[3–10]

Metal nanoparticles (MNPs) are especially attractive in the chemoselective reductions of aromatic carbonyl compounds and nitroarenes, using environmentally benign hydrogen sources.[11–13] Ligand-stabilized MNPs (amines, phosphines, thiolates, NHCs) improve the catalytic activity and chemoselectivity as well.[14–17] RhNPs have shown that surface modification using P-donor ligands as stabilizers enhance the chemoselectivity of the reduction of arenes with H_2; however, bulky P-donor ligands reduce conversion rates.[18–22]

RhNPs catalysts in ionic liquids control the selectivity towards phenylethanol in the reduction of acetophenone. Although high selectivity of phenylethanol was achieved at low conversion for RhNPs in [BMIM][PF_6], when the reaction was carried out to completion, the selectivity diminished.[23] It has been reported that bipyridine (bipy) ligands enhance the stability and the catalytic performance of RhNPs in imidazolium-based ILs, obtaining low selectivity to 1-phenylethanol in the reduction of acetophenone with 2,2'-bipyridine as ligand.[24] Rh/bipy ratio was important to control the selectivity of RhNPs in this process. It has been proposed that the rate-determining step in hydrogenation of arenes is the decoordination of bipy from the nanoparticle surface.[25] The rational design of ancillary stabilizers that contain bipyridine and imidazolium groups had remarkable impact on the activity and selectivity of RhNPs. The ancillary ligand affords the proper stabilization of RhNPs and at the same time the formation of ligand-free RhNPs surface.[25] In our recent work, thiolate-stabilized RhNPs in the ionic liquid [BMIM][BF_4], showed selectivity towards the reduction of alkene, nitro and imine groups of aromatic substrates, and in the *N*-reductive alkylation of nitrobenzene and benzaldehyde.[26]

As an alternative to the hydrogenation with molecular hydrogen, the catalytic transfer hydrogenation (TH) has received special attention due to the simplicity of the equipment and the selectivity control.[27,28] The use of formic acid as hydrogen source is environmentally preferable, since it can be produced from biomass in large scale and CO_2 is formed as byproduct during the TH reaction.[29,30] Many MNPs supported catalysts have been developed for the TH of nitroarenes; however, to attain high yields, long reaction times and complex supports are required.[31–37]

Herein, RhNPs were synthesized in the ionic liquid [BMIM][BF_4] and stabilized with pyridines to enhance its catalytic performance in the reduction of arylketones and nitroarenes. The catalytic systems RhNPs/Py/[BMIM][BF_4] were applied on the hydrogenation of arylketones with H_2, as well as in the hydrogen transfer reactions for the selective reduction of nitroarenes and in multistep reactions using formic acid-Et_3N azeotrope as hydrogen source.

Results and Discussion

Synthesis of Pyridine-stabilized RhNPs in [BMIM][BF_4]

Pyridine-stabilized RhNPs (**RhNPs-I**) were synthetized by decomposition of the organometallic precursor [Rh(μ-OMe)(COD)]$_2$ under reductive H_2 atmosphere, using one equivalent of pyridine as nanoparticles stabilizer and the ionic liquid [BMIM][BF_4] as solvent. A pressure of 10 bar and 80°C

[a] M. Sc. A. Serrano-Maldonado, Dr. Erika Martin, Dr. I. Guerrero-Ríos
Departamento de Química Inorgánica, Facultad de Química,
Universidad Nacional Autónoma de México,
Av. Universidad 3000, 04510 CDMX, Mexico
E-mail: itzelgr@unam.mx

Supporting information for this article is given via a link at the end of the document.

10.1002/ejic.201900223

during 18 h was required to carry out the complete reduction of the Rh precursor (figure 1) to the desired RhNPs together with cyclooctane and methanol as organic byproducts. When RhNPs were synthesized with 0.2 equivalents of Py, only rhodium agglomerates were observed (Supporting Information, figure S1).

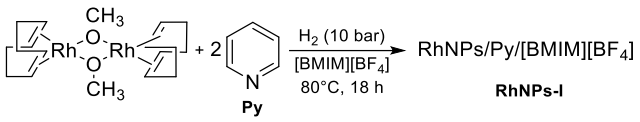

Figure 1. Synthesis of pyridine-stabilized RhNPs in [BMIM][BF_4].

The system **RhNPs-I** was characterized by HAADF-STEM (figure 2), revealing pseudo-spherical nanoparticles with a narrow size distribution of 2.8±0.4 nm for 400 nanoparticles (Supporting Information, figures S2). High-resolution images of a single nanoparticle showed interplanar distances of 2.2 Å, corresponding to the crystallographic planes (111) of Rh with fcc structure (figure 2). EDX analysis evidenced the presence of Rh (Supporting Information, figures S2).

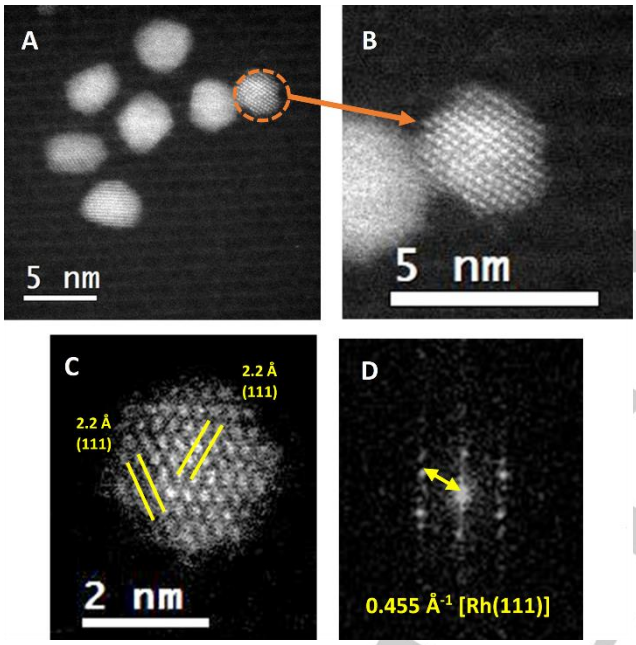

Figure 2. HR HAADF-STEM image of **RhNPs-I** (A); magnification of circled zone (B); HR HAADF-STEM image of a single Rh nanoparticle with atom-resolved structure, interplanar distances of 2.2 Å (111) (C); crystallographic plane spots observed by FFT of C (0.455 Å-1) (D).

XPS characterization of **RhNPs-I** was performed to identify rhodium species at the nanoparticle surface, revealing the presence of Rh together with N and F (Supporting Information, figure S3), indicative of the presence of pyridine stabilizer and ionic liquid as well. Deconvolution analysis of HR-XPS for Rh 3d showed only the presence of Rh(0) at the surface (figure 3A), neglecting the formation of oxides on the surface, due to the stabilization of ionic liquid. In the case of HR-XPS of N 1s, only one species at 398.43 eV was observed, that corresponded to the coordinated pyridine (figure 3B).

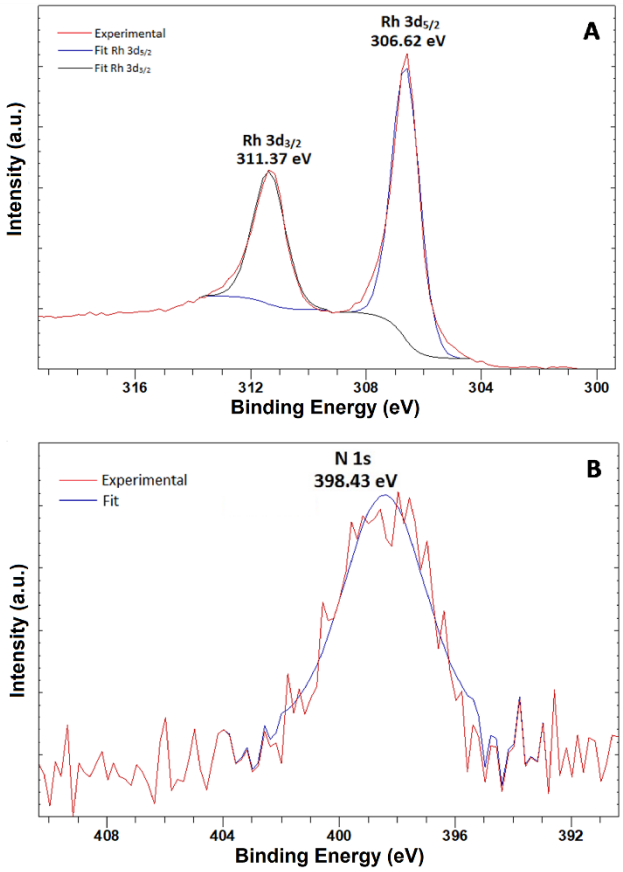

Figure 3. HR-XPS spectra for Rh 3d region (A) and N 1s region (B)

Further evidence of the presence of pyridine stabilizer was confirmed by TGA, where a mass loss around 205°C, corresponding to the total pyridine added during the RhNPs synthesis (Supporting Information, figure S6), points at a strong interaction of pyridine not only with the nanoparticle surface, but also with the ionic liquid.

RhNPs stabilized by 4-trifluoromethylpyridine (**RhNPs-II**), 4-*tert*-butylpyridine (**RhNPs-III**), and 4-(3-phenylpropyl)pyridine (**RhNPs-IV**) were synthesized in the ionic liquid [BMIM][BF_4]. TEM analyses (figure 4) showed spherical nanoparticles and narrow size distributions with similar size (3.0 – 3.4 nm, figures S7-S9) for all the systems (**RhNPs-II, III, IV**) and in comparison with **RhNPs-I**, larger nanoparticles were obtained with the substituted pyridine stabilizers. **RhNPs-III** with 4-*tert*-butylpyridine as stabilizer showed a tendency to agglomerate probably due to the presence of bulky groups in the stabilizer that hamper a good NPs dispersion. The absence of pyridine as previously shown for RhNPs in [BMIM][BF_4][26] generated nanoparticles with a mean diameter of 5.2±0.8 nm, clearly showing an effect of the stabilizer on the size control.

10.1002/ejic.201900223

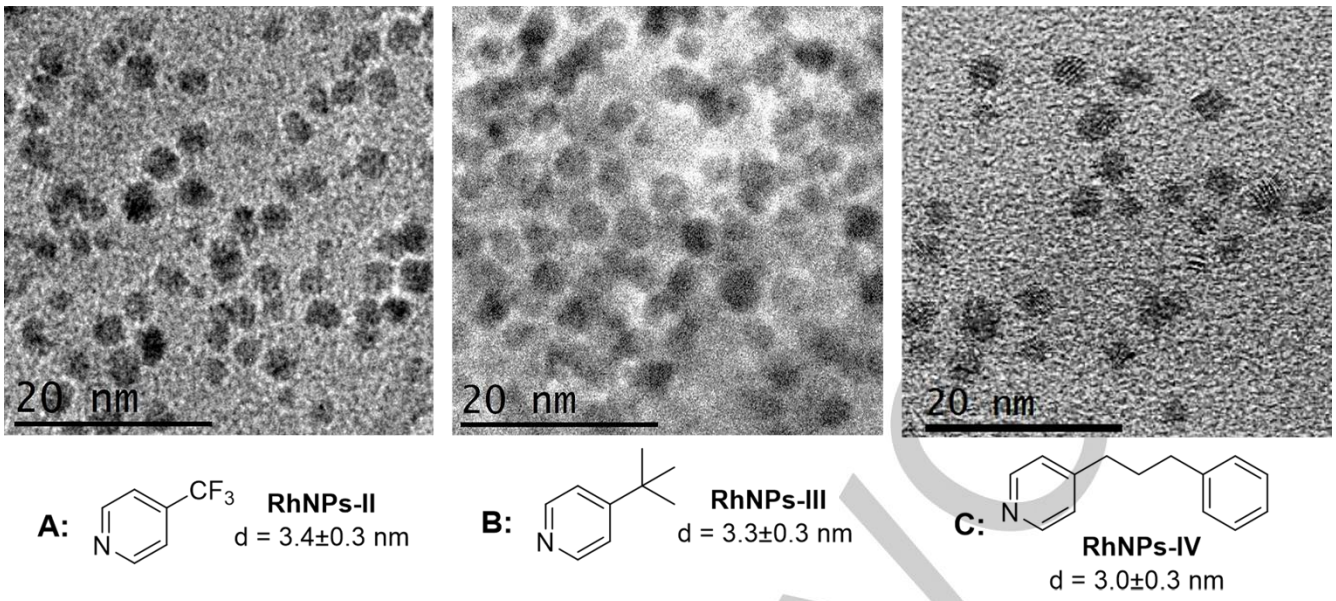

Figure 4. TEM images of **RhNPs-II** (A), **RhNPs-III** (B) and **RhNPs-IV** (C).

Table 1. Hydrogenation of acetophenone (**1**) catalyzed by RhNPs in [BMIM][BF_4].

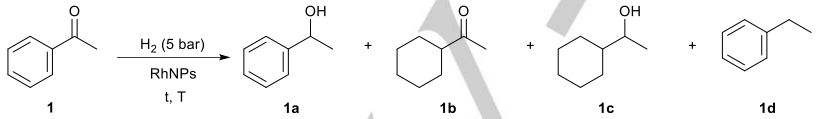

Entry	Catalytic system	Substrate (mmol)	Time (h)	Temperature (^{0}C)	% Conversion[a]	% Selectivity[a]			
						1a	1b	1c	1d
1	**RhNPs-I**	1	1	80	66	97	2	1	<1
2	**RhNPs-I**	1	1.5	80	81	90	2	7	1
3	**RhNPs-I**	1	1	100	87	89	3	7	1
4	**RhNPs-II**	1	1	100	86	78	5	10	7
5	**RhNPs-III**	1	1	100	85	84	5	9	2
6	**RhNPs-IV**	1	1	100	89	89	3	7	1
7[b]	**RhNPs-V**	1	1	100	52	95	2	2	1
8[b]	**RhNPs-V**	1	2	100	58	94	3	2	1
9	**RhNPs-I**	0.5	1	100	93	62	7	23	8
10	**RhNPs-I**	2	1	100	91	92	2	4	2
11	**RhNPs-I**	5	1	100	89	95	2	2	1
12	**RhNPs-I**	10	1	100	55	99	<1	<1	<1
13[c]	**RhNPs-bipy**[24]	1	15	80	70	38	22	40	0
14[d]	**RhNPs-(SR)**[26]	1	1	80	0	-	-	-	-

Results from duplicated experiments. Reaction conditions: 1 mL of the catalytic solution of RhNPs (10^{-2} mol L^{-1}, 0.01 mmol of total Rh), H_2 (5 bar), 1 h. [a] Determined by GC using *n*-decane as internal standard. [b] agglomeration of nanoparticles was observed at the end of reaction. [c] From ref. [24], using 40 bar H_2 pressure. [d] From ref. [26], using 50 bar H_2 pressure

Hydrogenation of acetophenones

The synthesized RhNPs, were evaluated in the reduction of acetophenone (**1**) with dihydrogen and the results are summarized in Table 1. Among the possible products expected for the reduction of **1** (scheme in Table 1), the selective hydrogenation of ketone could lead to phenylethanol (**1a**), of aromatic ring to acetylcyclohexane (**1b**), complete hydrogenation to cyclohexylethanol (**1c**), and the hydrogenolysis reaction of **1a** to ethyl benzene (**1d**) as side reaction.

When **RhNPs-I** were evaluated in the hydrogenation of **1** at 80°C and 1 h reaction time (table 1, entry 1), 97% selectivity to phenylethanol (**1a**) was observed with 66% of conversion. Increasing the reaction time further half hour (entry 2, table 1), increased the conversion to 81% but decreased the selectivity to **1a** (90%), due to the formation of **1c** (7%) at expenses of **1a**. Increasing the temperature to 100°C at 1 h reaction time (entry 3,

10.1002/ejic.201900223

table 1), increased the conversion to 87% with an 89% selectivity to **1a** and 7% to **1c**.

The RhNPs stabilized with different pyridines were also evaluated in the hydrogenation of **1**. Electron withdrawing substituents on the stabilizer 4-trifluoromethylpyridine in **RhNPs-II** reduce the selectivity to product phenylethanol **1a** (78%) in comparison with **RhNPs-I** (entry 4 vs entry 3, table 1). The minor binding strength of 4-trifluoromethylpyridine in **RhNPs-II**, favors ring hydrogenation as observed by Dyson *et al.* in the hydrogenation of toluene with different substituted bipiridynes used as stabilizers for RhNPs.[25] When pyridines with sterically demanding groups were used as stabilizers in **RhNPs-III** (4-tertbutylpyridine) and in **RhNPs-IV** (4-(3-phenylpropyl)pyridine) (entries 5 and 6, table 1), similar activities and selectivities compared to **RhNPs-I** were observed. The absence of pyridine stabilizers on RhNPs affected the catalytic performances as shown by **RhNPs-V** (entries 7 and 8 in table 1) that reached 58% conversion with high selectivity to **1a**. Formation of agglomerates was observed at the end of the catalytic reactions catalyzed with **RhNPs-V**, accounting for the low activity attained. The results suggested the beneficial effect of pyridine as stabilizer of RhNPs to avoid nanoparticles agglomeration and to obtain high conversion and selectivity.

The concentration of substrate affected the selectivity of products in the reactions catalyzed by **RhNPs-I** (entries 9-12 in table 1). At low concentration of substrate (entry 9, table 1), we observed higher conversion (93%) and lower selectivity towards phenylethanol (**1a**) (62%) with higher concentration of cyclohexylethanol (**1c**) (23%). Increasing the amount of acetophenone (**1**) to 2 mmol (entry 10, table 1), increased the selectivity (92%) to **1a** with a good conversion (91%). Further increment of substrate **1** to 5 and 10 mmol (entries 13 and 12, table 1) increased the selectivity to product **1a** to 98% but at higher concentration of substrate the conversion was diminished to 55%. The above results indicated that the reduction of carbonyl is much faster than that of the aromatic ring (product **1a** vs **1c**) and formation of **1c** is competitive when the substrate **1** is consumed. The pyridine stabilized **RhNPs-I** of this work (entries 1-2, table 1), showed a remarkable activity and selectivity compared to bipyridine stabilized RhNPs[24] (entry 13, table 1) and thiolate-capped RhNPs[26] (entry 14, table 1). The higher activity observed by **RhNPs-I** at similar rhodium concentration and rhodium:donor atom ratio (nitrogen or sulphur), could be accounted for the stronger binding strength of bipyridine and thiolate to rhodium.

To further study the influence of substrate and product concentration on the kinetics of the reaction, the hydrogenation reaction of acetophenone catalyzed by **RhNPs-I** was monitored during 2 h (figure 5, entries 1-4, table S1). At high concentrations of acetophenone (**1**), the reduction proceeds fast obtaining phenylethanol (**1a**) selectively. With a low concentration of **1**, the reaction is slower and the concentration of products, cyclohexylethanol (**1c**) and ethyl benzene (**1d**), increased due to the reduction of **1a**. The latter is a slow process as shown by the direct reduction of **1a** (Supporting Information, figure S12), where only 31% of conversion was observed with 77% selectivity of **1c** in 1 h. Regarding the path in which product **1c** is generated, it is possible to discard the direct reduction of acetylcyclohexane (**1b**), as shown by the low concentration observed of **1b** during the monitoring experiment, and by an independent experiment of the hydrogenation of **1b** (Supporting Information, figure S13), where no products were detected. This behavior agrees with previous reports where the coordination of substrate to the surface of nanoparticle forming di-σ-bonded species is necessary to carry out the hydrogenation of substrates.[22,38] Furthermore, evidence of heterogenous catalytic behavior by **RhNPs-I** was confirmed by addition of Hg(0) after a 15 min catalytic run, when the reaction turnover was inhibited (entries 5-6, table S1).[39] Considering these results, two possible reaction pathways were observed: route 1, wherein the ketone is reduced to form phenylethanol (**1a**); and route 2, wherein the aromatic ring was reduced to obtain cyclohexenone (**1b**) (figure 6). The products cyclohexylethanol (**1c**) and ethylbenzene (**1d**) can be obtained only from **1a**.

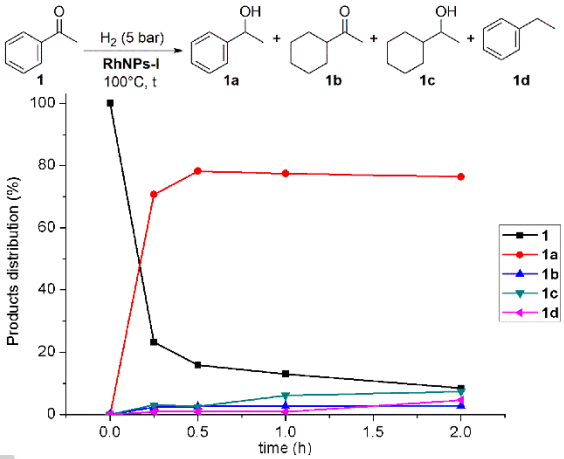

Figure 5. Monitoring of acetophenone hydrogenation catalyzed by **RhNPs-I**. Reaction conditions: 1 mmol of acetophenone (**1**) and 1 mL of the catalytic solution of RhNPs (10^{-2} mol L^{-1}, 0.01 mmol of total Rh), H_2 (5 bar), 100°C. Conversion and selectivity determined by GC using *n*-decane as internal standard.

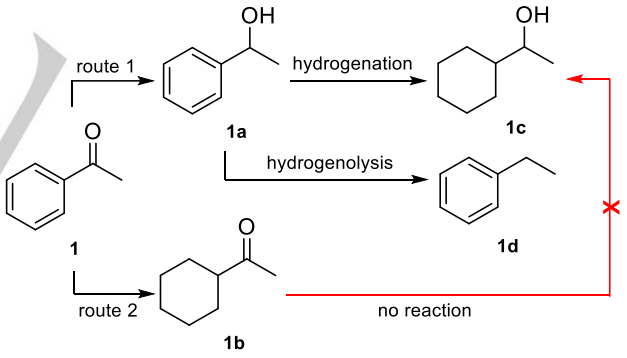

Figure 6. Hydrogenation pathways of acetophenone (**1**) catalyzed by RhNPs.

Recycling studies were carried out employing the catalytic system **RhNPs-I** and 2 mmol of acetophenone (**1**). After separation of products, the catalytic system was reused for up to ten runs without important loss of activity and selectivity, demonstrating that the catalytic system is robust and stable (figure 7). After the tenth catalytic run, the conversion amounted to 85% with 85% selectivity to phenylethanol (**1a**). Loss of activity and selectivity due to loss of rhodium was excluded by ICP-MS analysis of organic extracts. TEM analysis of **RhNPs-I** after the tenth catalytic run, evidenced agglomeration of nanoparticles (**figure S11**) that could account for the reduced activity and selectivity observed in the recycling experiments.

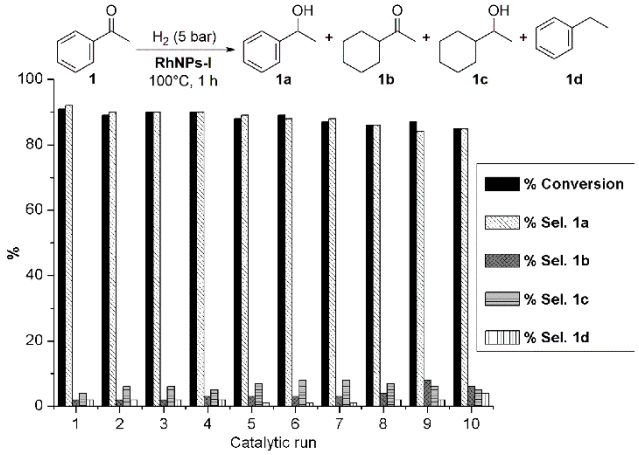

Figure 7. Recycling experiments of **RhNPs-I** in the hydrogenation of acetophenone (**1**). Reaction conditions: 2 mmol of acetophenone (**1**) and 1 mL of the catalytic solution of **RhNPs-I** (10^{-2} mol L^{-1}, 0.01 mmol of total Rh), H_2 (5 bar), 100°C, 1 h. Conversion and selectivity determined by GC using *n*-decane as internal standard.

The catalytic system **RhNPs-I** was applied in the reduction of substituted aryl ketones (substrates **2**-**8**, figure 8), achieving lower conversion compared to acetophenone **1**, with high selectivity to the corresponding aryl alcohol. The presence of a substituent in the aromatic ring limits the planar coordination of the substrate to the nanoparticle surface, minimizing ring hydrogenation and decreasing conversion. Electron-withdrawing group trifluoromethyl on aryl ketones (substrates **2** and **3**, figure 8) promoted the hydrogenation of the aromatic ring (10%) with conversions of 63% when *para*-substituted substrates were used, and 73% with *meta*-substituted substrates. Electron donor substituents on substrate **4** (figure 8) showed complete selectivity to the corresponding arylic alcohol with low conversion (34%) due to the inductive effect of methoxy groups. Substrates with methyl substituent in *para* and *ortho* positions (**5** and **6**, figure 8) that could affect the activity due to a possible steric effect, showed similar activity and selectivity; however, when the aromatic ring was *para*-substituted with a bulky group (**7**, figure 8), the conversion decreased to 11%. The substrate 4-*iso*-butylacetophenone (**8**, figure 8), an intermediate in the ibuprofen synthesis, was hydrogenated with high selectivity and moderate conversion (62%) to the corresponding alcohol. Varying the steric effect over the ketone group with substrates propiophenone (**9**, figure 8) and benzophenone (**10**, figure 8), affected moderately the activity and decreased the selectivity to alcohol. The reduction of non-conjugated aryl ketones (**11** and **12**, figure 8) were also tested, observing an important decrease in conversion and selectivity. Benzaldehyde (**13**, figure 8) was also employed as substrate working under the same reaction conditions, obtaining only 9% of conversion. An increase in the pressure of H_2 to 30 bar and 6 h reaction time were necessary to obtain 95% of conversion with 97% of selectivity to benzylic alcohol (Supporting Information, table S3). Interestingly, when the reaction was carried out adding 0.5 mL of acetone at 5 bar of H_2 pressure during 1 h, the conversion increased to 53%, suggesting that the low conversion of **13** is limited by low diffusion in the ionic liquid.

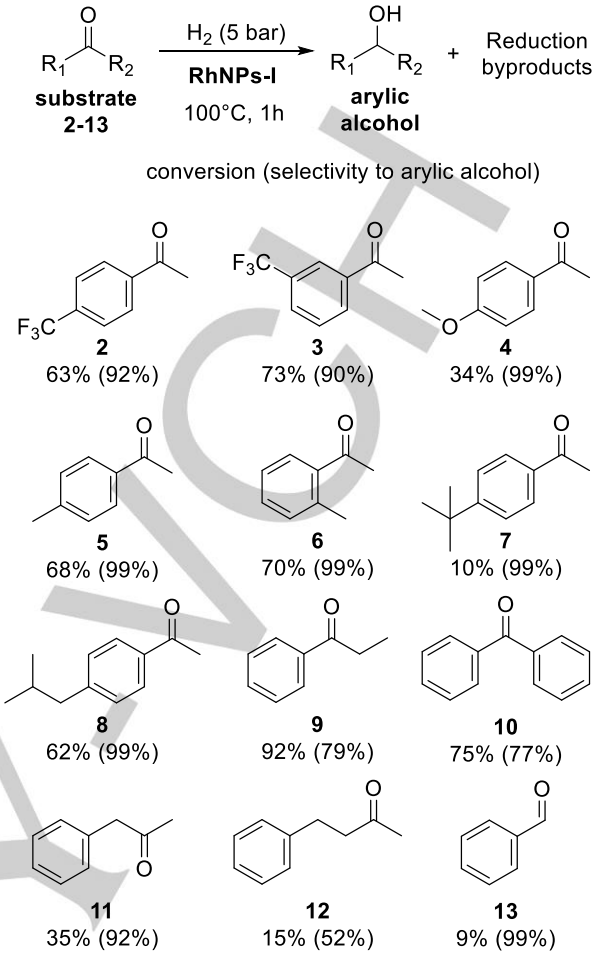

Figure 8. Scope of reaction. Reaction conditions: 1 mmol of substrate and 1 mL of the catalytic solution of **RhNPs-I** (10^{-2} mol L^{-1}, 0.01 mmol of total Rh), H_2 5 bar), 100°C, 1 h. Conversion and selectivity determined by GC using *n*-decane as internal standard.

Transfer hydrogenation of nitrobenzene and imine derivatives

The catalytic reduction of nitrobenzene to selectively obtain aniline, an important building block of many compounds, was tested under the reaction conditions used for the reduction of aryl ketones with the catalytic system **RhNPs-I** (figure 9). Working under these conditions, 62% conversion and 90% selectivity to aniline (**14a**) were obtained.

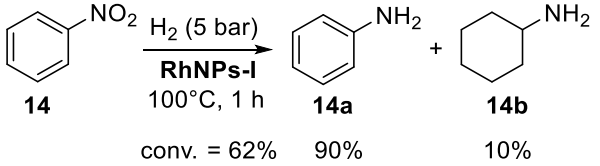

Figure 9. **RhNPs-I** catalyzed nitrobenzene reduction with dihydrogen. Reaction conditions: 1 mmol of substrate and 1 mL of the catalytic solution of **RhNPs-I** 10^{-2} mol L^{-1}, 0.01 mmol of total Rh). Conversion and selectivity determined by GC using *n*-decane as internal standard.

To improve the selectivity and activity in the reduction of nitroarenes, another source of hydrogen was studied. The use of formic acid-Et_3N azeotrope for transfer hydrogenation reactions (TH) have been used for the reduction of nitroarenes to anilines with several supported nanoparticle catalysts (metal or metal

10.1002/ejic.201900223

oxides), with high activity and selectivity.[35,37,40] The reduction of nitrobenzene (**14**) catalyzed by the system **RhNPs-I**, under TH conditions was completed in only 5 min, with total selectivity to aniline (**14a**) (entry 1, table 2) in simple reflux reaction conditions. The reaction did not proceed when a less reactive substrate as nitrodecane (**15**) was used.

Table 2. RhNPs-I catalyzed transfer hydrogenation with HCOOH

Entry	Substrate	Product	Conversion[a]	Time (min)
1	 **14**	 **14a**	>99	5
2	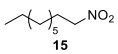 **15**	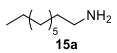 **15a**	0	60
3	 **1**	 **1a**	0	60
4	 **13**	 **13a**	0	60
5[b]	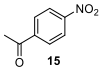 **15**	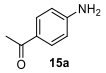 **15a**	>99	5

Results from duplicated experiments. Reaction conditions: 1 mmol of substrate and 1 mL of the catalytic solution of RhNPs-I (10^{-2} mol L^{-1}, 0.01 mmol of total Rh), 5 eq. of HCOOH/NEt_3 (5:2), 100°C. [a] Determined by GC using *n*-decane as internal standard. [b] Conversion determined by ^{1}H NMR.

Under similar conditions, the reduction of acetophenone (**1**) or benzaldehyde (**9**) (entries 3 and 4, table 2), was not possible, and when 4-nitroacetophenone (**15**) was used as substrate (entry 5, table 2), complete conversion to 4-acetylaniline (**15a**) was obtained. The results indicate that transfer hydrogenation with formic acid-Et_3N catalyzed by **RhNPs-I** is highly active and selective to nitrobenzene reduction. The latter suggests a different mechanism for transfer hydrogenation reaction for nitroarenes compared to the one observed in the hydrogenation of acetophenone (see above).

Considering the selectivity to nitroarenes of **RhNPs-I** in the transfer hydrogenation reaction, the one pot synthesis of N-benzylamine (**16a**) through the reductive *N*-alkylation of nitrobenzene (**14**) and benzaldehyde (**13**) was studied under these reaction conditions. The reaction proceeds through three steps: a) reduction of **14** to aniline (**14a**); b) condensation of **14a** with **13** to form *N*-benzylidenaniline (**17**); and c) hydrogenation of **17** to *N*-benzylaniline (**17a**). To attain high selectivity to amine the amount of formic acid-Et_3N azeotrope was increased to 10 equivalents at 120°C and 2 h reaction time (entry 1, table 3). Under these reaction conditions **RhNPs-I** afforded complete conversion and 91% selectivity to **17a**. Furthermore, reducing Rh concentration to 0.1 mol % (entry 2, table 3) resulted in complete conversion and 95% selectivity to **17a**. To our knowledge, this nanoparticle-based catalyst is one of the most active systems reported.

The *N*-reductive alkylation was also studied with substituted benzaldehydes *p*-anisaldehyde (**18**) and 4-chlorobenzaldehyde (**19**). When the reactions were carried out with a Rh concentration of 1 mol %, complete conversion was observed with high selectivity to amines **20a** and **21a** (entries 3 and 5, table 3). However, when the Rh concentration was decreased to 0.1 mol %, the conversion was only 30% of substrate **18** and 48% of **19**. The reduction of imine to amine was also lower, with 48% of amine with **18** and 59% of amine with **19** (entries 4 and 6, table 3). The decay in activity for aldehydes **18** and **19** in comparison with the reaction using benzaldehyde **13**, was probably due to the interaction of chloride and methoxy substituents with the nanoparticle surface, hampering the hydrogenation of nitrobenzene (**14**).

Table 3. RhNPs-I catalyzed *N*-reductive alkylation by transfer hydrogenation with HCOOH

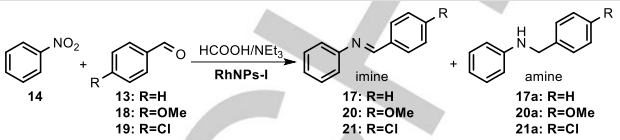

14 — **13**: R=H, **18**: R=OMe, **19**: R=Cl — **17**: R=H, **20**: R=OMe, **21**: R=Cl — **17a**: R=H, **20a**: R=OMe, **21a**: R=Cl

Entry	Aldehyde	[Rh] (mol %)	Conversion (%)[a]	imine/amine (%)[a]
1	**13**	1	99	9/91
2	**13**	0.1	99	5/95
3	**18**	1	99	10/90
4	**18**	0.1	30	52/48
5	**19**	1	99	7/93
6	**19**	0.1	48	41/59

Results from duplicated experiments. Reaction conditions: 1 mmol of nitrobenzene (**14**) and 1 mmol of selected benzaldehyde; 1 mL of the catalytic solution of **RhNPs-I** (10^{-2} mol L^{-1}, 0.01 mmol of total Rh), 10 eq. of HCOOH/NEt_3 (5:2), 120°C. 2h. [a] Determined by GC using *n*-decane as internal standard.

Pyrrole synthesis through a nitroarene reduction and Paal-Knorr condensation

Pyrrole ring is a heterocycle present in a large variety of biological active alkaloids, with a wide range of applications in the synthesis of drugs, pigments, conducting materials and electroluminescence devices.[41] The Paal-Knorr reaction is a route to obtain pyrroles and consists in the condensation between a 1,4-dicarbonyl compound and a primary amine under acidic conditions. Considering the activity of **RhNPs-I** in the nitrobenzene reduction by transfer hydrogenation with formic acid-Et_3N azeotrope (see above), we carried out a tandem process to prepare *N*-substituted aryl pyrroles starting from nitroarene and 2,5-hexanodione with this catalytic system. The reaction proceeds in two steps: a) nitroarene (**14** or **16**) reduction to the corresponding aniline; b) condensation between aniline (**14a** or **16a**) and 2,5-hexanedione (**22**) to form the corresponding pyrrole under acidic conditions provided by the presence of formic acid. When nitrobenzene (**14**) was used as substrate, the reaction proceeded with 92% yield of the corresponding pyrrole (**23**) (figure 10). When 4-nitroacetophenone (**16**) was used as substrate, the yield is reduced to 69%, probably due to low diffusion of intermediate products. This strategy showed good yields at short reaction times and is completely selective to the pyrrole since the presence of pyrrolidine was not observed.

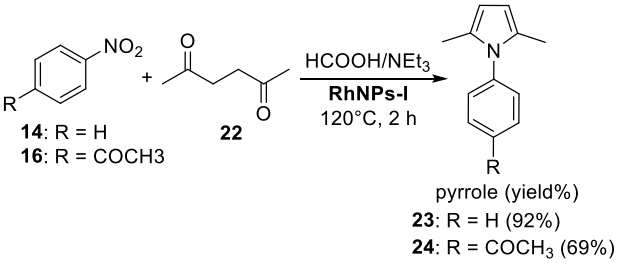

Figure 10. RhNPs-I catalyzed tandem nitroarene reduction/Paal Knorr condensation. Reaction conditions: 1 mmol of nitroarene, 1 mmol of 2,5-hexanedione (**22**), 100 μl of the catalytic solution of **RhNPs-I** (0.001 mmol of total Rh), 10 eq. of HCOOH/NEt_3 (5:2). Yield determined by GC and ^{1}H NMR.

10.1002/ejic.201900223

Conclusions

In summary, we found that the use of pyridine derivatives as stabilizers during the synthesis of rhodium nanoparticles in ionic liquid [BMIM][BF_4] generated well-dispersed systems of RhNPs with small diameter (2.8-3.4 nm).

The systems catalyze the hydrogenation of acetophenone, where the pyridine stabilized nanoparticles **RhNPs-I** showed the best activity and selectivity to phenylethanol. **RhNPs-V** without pyridine stabilizer showed low activity due to the formation of inactive agglomerates on the reaction conditions used. For pyridine-stabilized RhNPs, the reduction of aromatic ring is slower than ketone reduction thus favoring the selectivity to arylic alcohol. The catalytic system was reused for up to ten runs without loss of activity and selectivity.

RhNPs-I showed good selectivity for the reduction of substituted arylketones to the corresponding alcohol, where bulky substituents in the aromatic ring hampered reduction. In addition, substrates with non-conjugate ketone groups hinder the formation of di-σ-bonded species on the nanoparticle surface, diminishing ketone reduction.

The reduction of nitroarenes to the corresponding aniline by **RhNPs-I** with dihydrogen showed moderate activity and selectivity, whereas the transfer hydrogenation using formic acid-Et_3N azeotrope showed remarkable activity in the reduction of nitroarenes. Under transfer hydrogenation conditions, the acetophenone was not transformed suggesting a different reduction mechanism.

The versatility of the catalytic system allowed the application in multistep processes, such as the *N*-reductive alkylation to form substituted anilines, and the sequential nitroarene reduction followed by Paal-Knorr condensation to generate substituted pyrroles. An advantage of these reactions is that no specialized equipment is needed (autoclaves, reactors), since the multistep reactions can be performed in a simple reflux system.

Experimental Section

General

All manipulations were carried out in a dry, oxygen-free nitrogen atmosphere using standard Schlenk techniques. Ionic liquid was dried under vacuum (0.05 mmHg) at 60°C for 18 h before use. All reagents were acquired from commercial suppliers; benzaldehyde were purified according to reported methods prior to use,[42] and the rest of reagents were used as received. Ionic liquid 1-butyl-3-methylimidazolium tetrafluoroborate ([BMIM][BF_4]) (BASF grade) was purchased from Sigma-Aldrich. [Rh(μ-OMe)(COD)]$_2$ was synthesized following reported methods.[43] NMR were obtained on a Varian VNMRS spectrometer at 400 MHz for ^{1}H. Chemical shifts (δ) are given in ppm relative to residual solvent peak. Thermogravimetric analysis was performed on a Perkin Elmer TGA4000 system, employing a sample of RhNPs as prepared. Transmission electron microscopy for high resolution images were acquired on a JEOL ARM200F microscope with HAADF-STEM detector, and the rest of images were acquired on a JEOL JEM-2010 microscope with bright field detector. Nanoparticle diameter was determined counting at least 400 individual nanoparticles with the software package *Digimizer 4.6.1*.[44] Catalytic conversions were determined on a Varian 3800 gas chromatograph with a capillary column DB-Wax (30 m x 0.32 mm x 0.25 mm) coupled to a FID detector, using *n*-decane as internal standard. Synthesis of nanoparticles and catalytic hydrogenations were carried out on a Parr Multi Reactor 500 system with 25 mL reactor vessels. Catalytic transfer hydrogenations were carried out on a Radleys Carousel 12 Plus Reaction Station RR91023 with 5 mL glass tubes. ICP-MS experiments were performed on a Bruker Aurora M90 equipment, digesting the sample with nitric acid. XPS measurements were performed using a PHI 5000 VersaProbe II (from Physical Electronics), with an Al-Kα X-ray source ($h\nu$ = 1486.6 eV), a beam size of 100 μm, power of 25 W and X-ray voltage of 25 KV. XPS spectra were obtained at 45° from the normal surface in the constant pass energy mode (CAE), E_0 = 117.3 eV and 23.5 eV for survey and high-resolution narrow scan with a step size of 1 eV and 0.2 eV respectively. Peak positions were referenced to the Shirley background Ag $3d_{5/2}$ core level at 368.20 eV, Au $4f_{7/2}$ at 84.00 eV and C 1s hydrocarbon groups at 284.00 eV central peaks. Analyses were performed in ultra-high vacuum (10^{-8} mbar). XPS spectra were fitted with the program *CasaXPS*.[45] The assignment of chemical components of core level N 1s and Rh 3d were made using the referenced value reported in the literature.[46,47]

General synthesis of RhNPs in [BMIM][BF_4]. The precursor [Rh(μ-OMe)(COD)]$_2$ (0.025 mmol, 0.05 mmol of total Rh), the selected pyridine (0.05 mmol) and ionic liquid [BMIM][BF_4] (5 mL) were placed in a 25 mL stainless steel reactor vessel. The mixture was magnetically stirred and heated for 15 min at 70°C, followed by pressurization with H_2 (10 bar) and stirring for 18 h at 80°C. The reactor vessel was cooled to room temperature and depressurized. The resulting black homogeneous solution of dispersed nanoparticles was washed with hexanes (3 x 5 mL) to remove organic byproducts and dried under vacuum (0.05 mmHg) for 18 hours.

General procedure for catalytic hydrogenation with H_2. Dispersed RhNPs in ionic liquid (1 mL, 0.01 mmol of Rh) were placed in a 25 mL stainless steel reactor vessel together with the set amount of selected substrate and *n*-decane as internal standard (97 μl, 0.5 mmol). The reactor was pressurized with H_2 at the desired pressure, temperature and time. After the reaction was completed, the reactor vessel was cooled to room temperature and depressurized. Products were extracted with a solvent mixture of hexanes/toluene 10:1 (5 x 3 mL) and analyzed by gas chromatography by comparison with the commercial product. Hydrogenation of substituted acetophenones were also monitored by ^{1}H NMR.

Recycling experiments of catalytic hydrogenation. After products extraction, the catalytic phase (1 mL of **RhNPs-I**) was dried under vacuum at 80°C to remove volatiles for 3 h. Additional substrate and standard were added and the same procedure for hydrogenation reaction was followed. The presence of Rh in extracted products was discarded by ICP-MS.

General procedure for catalytic transfer hydrogenation and multistep processes. The set amount of dispersed RhNPs in ionic liquid were placed in a 5 mL reaction glass tube together with the substrate(s) (1 mmol) and *n*-decane as internal standard (97 μl, 0.5 mmol). The tube was heated to the set temperature and amount of the azeotrope HCOOH/NEt_3 (5:2) was added to start the reaction. After the reaction was completed, the reaction tube was cooled down with an ice bath. Products were extracted with a solvent mixture of hexanes/toluene 10:1 (5 x 3 mL) and analyzed by gas chromatography by comparison with the commercial product. *N*-reductive alkylation reactions with substituted aldehydes were monitored by ^{1}H-NMR.

Acknowledgements

This work was financially supported by the project DGAPA-PAPIIT IN226616 and IA205816. A.S.-M. thanks CONACyT for a PhD grant. Authors thank Dr. Salas-Martin for technical support. Special thanks for Dr. Zuñiga for helpful discussions.

Keywords: Rhodium nanoparticles • ionic liquids • selective reduction • transfer hydrogenation • multistep processes

[1] M. Guerrero, N. T. T. Chau, S. Noel, A. Denicourt-Nowicki, F. Hapiot, A. Roucoux, E. Monflier, K. Philippot, *Curr. Org. Chem.* **2013**, *17*, 364–399.

[2] Y. Yuan, N. Yan, P. J. Dyson, *ACS Catal.* **2012**, *2*, 1057–1069.

[3] S. A. Stratton, K. L. Luska, A. Moores, *Catal. Today* **2012**, *183*, 96–100.

[4] E. Redel, J. Krämer, R. Thomann, C. Janiak, *J. Organomet. Chem.* **2009**, *694*, 1069–1075.

[5] S. Wegner, C. Janiak, *Metal Nanoparticles in Ionic Liquids*, Springer International Publishing, **2017**.

[6] C. Janiak, *Zeitschrift fur Naturforsch. - Sect. B J. Chem. Sci.* **2013**, *68*, 1059–1089.

[7] D. Marquardt, C. Vollmer, R. Thomann, P. Steurer, R. Mülhaupt, E. Redel, C. Janiak, *Carbon N. Y.* **2011**, *49*, 1326–1332.

[8] J. Dupont, J. D. Scholten, *Chem. Soc. Rev.* **2010**, *39*, 1780.

[9] J. Dupont, L. Kollár, *Top. Organomet. Chem.* **2015**, *51*, 1.

[10] B. Léger, A. Denicourt-nowicki, H. Olivier-Bourbigou, A. Roucoux, *ChemSusChem* **2008**, *1*, 984–987.

[11] S. Sharma, D. Bhattacherjee, P. Das, *Adv. Synth. Catal.* **2018**, *360*, 2131–2137.

[12] J. W. Park, Y. K. Chung, *ACS Catal.* **2015**, *5*, 4846–4850.

[13] A. D. Verma, R. K. Mandal, I. Sinha, *RSC Adv.* **2016**, *6*, 103471–103477.

[14] F. Viñes, J. R. B. Gomes, F. Illas, *Chem. Soc. Rev.* **2014**, *43*, 4922–4939.

[15] D. J. Gavia, Y. S. Shon, *ChemCatChem* **2015**, *7*, 892–900.

[16] P. Lara, A. Suárez, V. Collière, K. Philippot, B. Chaudret, *ChemCatChem* **2014**, *6*, 87–90.

[17] M. J. Beier, J. M. Andanson, T. Mallat, F. Krumeich, A. Baiker, *ACS Catal.* **2012**, *2*, 337–340.

[18] J. L. Castelbou, P. Blondeau, C. Claver, C. Godard, *RSC Adv.* **2015**, *5*, 97036–97043.

[19] H. Y. Jiang, X. X. Zheng, *Appl. Catal. A Gen.* **2015**, *499*, 118–123.

[20] D. J. M. Snelders, N. Yan, W. Gan, G. Laurenczy, P. J. Dyson, *ACS Catal.* **2012**, *2*, 201–207.

[21] J. L. Castelbou, A. Gual, E. Mercadé, C. Claver, C. Godard, *Catal. Sci. Technol.* **2013**, *3*, 2828.

[22] J. L. Castelbou, E. Bresó-Femenia, P. Blondeau, B. Chaudret, S. Castillón, C. Claver, C. Godard, *ChemCatChem* **2014**, *6*, 3160–3168.

[23] F. Jutz, J. M. Andanson, A. Baiker, *J. Catal.* **2009**, *268*, 356–366.

[24] A. Denicourt-Nowicki, B. Léger, A. Roucoux, *Phys. Chem. Chem. Phys.* **2011**, *13*, 13510.

[25] R. R. Dykeman, Y. Yuan, N. Yan, H. Asakura, K. Teramura, T. Tanaka, P. J. Dyson, *ChemCatChem* **2012**, *4*, 1907–1910.

[26] A. Serrano-Maldonado, S. S. Rozenel, J. L. Jimenez-Santiago, I. Guerrero-Ríos, E. Martin, *Catal. Sci. Technol.* **2018**, *8*, 4373–4382.

[27] D. Wang, D. Astruc, *Chem. Rev.* **2015**, *115*, 6621–6686.

[28] L. Kong, J. Zhao, T. Cheng, J. Lin, G. Liu, *ACS Catal.* **2016**, *6*, 2244–2249.

[29] J. Reichert, B. Brunner, A. Jess, P. Wasserscheid, J. Albert, *Energy Environ. Sci.* **2015**, *8*, 2985–2990.

[30] J. Eppinger, K.-W. Huang, *ACS Energy Lett.* **2017**, *2*, 188–195.

[31] T. Schwob, R. Kempe, *Angew. Chemie - Int. Ed.* **2016**, *55*, 15175–15179.

[32] E. E. Drinkel, R. R. Campedelli, A. M. Manfredi, H. D. Fiedler, F. Nome, *J. Org. Chem.* **2014**, *79*, 2574–2579.

[33] Q. Zhang, S. S. Li, M. M. Zhu, Y. M. Liu, H. Y. He, Y. Cao, *Green Chem.* **2016**, *18*, 2507–2513.

[34] Y. Duan, T. Song, X. Dong, Y. Yang, *Green Chem.* **2018**, *20*, 2821–2828.

[35] P. Zhou, Z. Zhang, *ChemSusChem* **2017**, *10*, 1892–1897.

[36] L. Jiang, P. Zhou, Z. Zhang, S. Jin, Q. Chi, *Ind. Eng. Chem. Res.* **2017**, *56*, 12556–12565.

[37] F. Chen, B. Sahoo, C. Kreyenschulte, H. Lund, M. Zeng, L. He, K. Junge, M. Beller, *Chem. Sci.* **2017**, *8*, 6239–6246.

[38] J. S. Zhu, Y.-S. Shon, *Nanoscale* **2015**, *7*, 17786–17790.

[39] J. A. Widegren, M. A. Bennett, R. G. Finke, *J. Am. Chem. Soc.* **2003**, *125*, 10301–10310.

[40] F. Chen, A. E. Surkus, L. He, M. M. Pohl, J. Radnik, C. Topf, K. Junge, M. Beller, *J. Am. Chem. Soc.* **2015**, *137*, 11718–11724.

[41] V. Estévez, M. Villacampa, J. Carlos Menéndez, *Chem. Soc. Rev.* **2014**, *43*, 4633–4657.

[42] C. L. L. Armarego, W. L., & Chai, **2013**, 67–69.

[43] J. A. C. R. Uson, L. A. Oro, *Inorg. Synth.* **1985**, *23*, 126–130.

[44] *Digimizer 4.6.1*, MedCalc Software, Belgium, **2005-2012**.

[45] *CasaXPS*, V2.3, Casa Software Ltd, **1999-2015**. *CasaXPS*, V2.3, Casa Software Ltd, **1999-2015**.

[46] C. Jin, W. Xia, T. C. Nagaiah, J. Guo, X. Chen, N. Li, M. Bron, W. Schuhmann, M. Muhler, *J. Mater. Chem.* **2010**, *20*, 736.

[47] Y. Li, N. Li, K. Yanagisawa, X. Ding, X. Li, *J. Mater. Chem. A* **2014**, *2*, 1484–1492.

10.1002/ejic.201900223

WILEY-VCH

FULL PAPER

Pyridine-stabilized RhNPs in the ionic liquid [BMIM][BF_4] were evaluated in the reduction of arylketones and nitroarenes with dihydrogen and formic acid-Et_3N azeotrope, respectively. RhNPs were applied in the synthesis of amines and pyrroles under transfer hydrogenation conditions, through the sequential multistep processes *N*-reductive alkylation and nitroarene reduction/Paal-Knorr condensation.

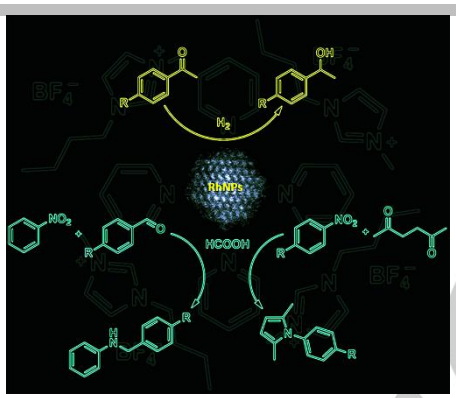

*Alejandro Serrano-Maldonado, Erika Martin, Itzel Guerrero-Ríos**

Page No. – Page No.

Pyridine-stabilized rhodium nanoparticles in ionic liquid as selective catalysts in hydrogenation and transfer hydrogenation processes.